

Chapter 6

Quasi-2D Turbulence in Shallow Fluid Layers



Herman J. H. Clercx

Abstract Flows in thin fluid layers, like in the Earth's atmosphere or oceans, tend to behave as quasi-two-dimensional flows. Their dynamics is strikingly different from three-dimensional flows, and main features of the flow dynamics can be understood by considering two-dimensional (2D) fluid flows. Inviscid 2D flows are governed by conservation of vorticity due to absence of vortex stretching and tilting. Together with conservation of kinetic energy this results in the famous inverse energy cascade and the emergence and persistence of large-scale vortices. This also occurs in shallow fluid-layer flows even if they are neither purely inviscid nor perfectly two-dimensional. Basic phenomena for understanding the dynamics of 2D flows will be discussed and 2D flows on bounded domains, mainly dealing with the large-scale phenomenology of the flow, will be addressed: the self-organization of 2D turbulence in confined domains and the interaction of coherent structures with domain walls. This will be complemented with some observations from recent experiments on quasi-2D turbulence in shallow-fluid layers including the role and impact of bottom friction and out-of-plane motion on the flow evolution.

6.1 Introduction

Large-scale geophysical flows in the oceans and in the atmosphere basically consist of a relatively thin fluid layer (with typical thickness \mathcal{H}) with a large horizontal extent, where we denote the horizontal length scale with $\mathcal{L} \gg \mathcal{H}$. Flow phenomena on horizontal scales much larger than the thickness of the fluid layer (typically a few kilometers deep in the oceans or 10 km high in the atmosphere) behave predominantly as two-dimensional (2D) flows. The common justification is that a small vertical

H. J. H. Clercx (✉)

Fluid Dynamics Laboratory, Department of Applied Physics, Eindhoven University of Technology, P.O. Box 513, 5600 Eindhoven, MB, The Netherlands
e-mail: h.j.h.clercx@tue.nl

© Springer Nature Switzerland AG 2022

H. Schuttelaars et al. (eds.), *The Mathematics of Marine Modelling*,
Mathematics of Planet Earth 9, https://doi.org/10.1007/978-3-031-09559-7_6

135

length scale implies small characteristic vertical velocities due to mass conservation. In shallow coastal seas, estuaries or shallow lakes with depths in the range of 10–100 m and horizontal extents of tens or hundreds of kilometers one can assume, based on similar arguments as above, quasi-2D behaviour of large-scale flows. Even on the level of riverine flows, aspects of the dynamics of large-scale eddies can be analysed invoking two-dimensionality, see Uijttewaal (2014) for a recent overview. Besides the aspect ratio of vertical and horizontal length scales some other mechanisms may contribute to the process of two-dimensionalization of the flow. It is known that background rotation promotes two-dimensionality which is nicely illustrated by the Taylor-Proudman theorem (Proudman 1916; Taylor 1917). This theorem basically states that for steady inviscid rapidly rotating flows the fluid velocity will not change in the direction parallel to the background rotation. In the oceans the rotation of the Earth will contribute to two-dimensionalization of large-scale flows with characteristic horizontal length scales larger than about 100 km at low latitudes, gradually decreasing to about 20 km at high latitudes, and in the atmosphere for flow scales with a horizontal extent larger than typically 1000 km. In shallow coastal seas, estuarine flows or lakes a stable density stratification (by salinity or temperature effects or a combination of them) suppresses vertical motion as that would enhance potential energy content of the flow. Such flows have also a tendency to move predominantly in the horizontal plane, thus contributing to quasi-two-dimensionality of the flow. Note, however, that the type of two-dimensional flow is different depending on the mechanism enforcing it: shallow and stratified flows tend to be flat because of the constraints in the vertical while background rotation forms tall vertically-invariant columnar structures. This leads to competing effects when combining rotation with either shallowness or stratification; see, for example, Liechtenstein et al. (2005), Duran-Matute et al. (2012).

Also the presence of domain boundaries might be important. Consider, for example, closed or semi-closed basins such as the Gulf of California, the Gulf of Aden, or in the Mediterranean the Adriatic or Tyrrhenian Sea. They reveal the existence of arrays of vortical structures. A nice illustration of the flow in the Gulf of Aden, visualized by phytoplankton blooms, is shown in Fig. 6.1. We can indeed observe relatively large flow structures, including vortices with size almost the same as the width of the Gulf of Aden. Similar patterns have been observed for the Adriatic Sea, as reported by Falco et al. (2000), and for the Tyrrhenian Sea a few years earlier by Buffoni et al. (1997). The energy to drive such vortical flows is mostly supplied by the wind. Of course, one will never observe a perfect array of vortices as the wind varies, the coastal boundaries are irregular and the bottom topography affects the flow. Nevertheless, the basic flow phenomena, including the formation of arrays of domain-sized vortices is inherently related to the self-organization of 2D turbulent flows in confined (rectangular) geometries. Moreover, such arrays of vortices interact with domain boundaries, or are perturbed otherwise, inducing unsteady wiggling of these vortices. Such processes can lead to efficient transport and mixing of passive tracers (such as nutrients or salt) or inertial particles.

The quasi-two-dimensionality of many geophysical and environmental flows inspired research on the behaviour of 2D flows, including vortex dynamics and 2D



Fig. 6.1 A winter plankton bloom in the Gulf of Aden. In the image the swirling motion of the phytoplankton bloom in the basin-wide vortical structures is clearly visible. The image is composed of data acquired on February 12, 2018, by the MODIS on the Aqua Satellite of NASA. Credit NASA image by Norman Kuring, NASA's Ocean Biology Processing Group. Photograph courtesy of Joaquim Goes, Lamont Doherty Earth Observatory

turbulence. A few examples of studies motivated by environmental flows include turbulent wakes, large-scale flow structures and mixing processes in shallow flows (Chen and Jirka 1995; Uijttewaal and Booij 2000; Jirka 2001), grid-generated turbulence in a shallow fluid layer by Uijttewaal and Jirka (2003), and the dynamical behavior of monopolar and dipolar vortices in such shallow turbulent flows, see Lin et al. (2003), Sous et al. (2004), Sous et al. (2005). It has also motivated studies of the mechanisms promoting two-dimensionality by, for example, background rotation or density stratification. Regarding the fundamental aspects of (2D) turbulence, the reduction of dimensionality already attracted a lot of attention from a wide variety of scientists. These investigations have been of theoretical and numerical character, where two-dimensionality facilitates analysis and computations significantly by exploiting the reduction of dimensionality (2D instead of 3D computations, for some recent reviews with regard to numerical studies, see Clercx and Van Heijst (2009), Boffetta and Ecke (2012)), but also laboratory experiments turned out to be extremely worthwhile as such flows are easily accessible for flow diagnostics. The dynamics of vortices can be studied in rotating or density-stratified fluids, see the review by Van Heijst and Clercx (2009), and 2D turbulence can be studied experimentally in density stratified fluids, in shallow fluid layer experiments or in soap film experiments, see Danilov and Gurarie (2000), Tabeling (2002), Kellay and Goldburg (2002), Van Heijst et al. (2006), Van Heijst and Clercx (2009), Clercx and Van Heijst (2009).

In this chapter the focus will be on the large-scale flow phenomenology. It will start with a brief overview of the basic mechanisms in unbounded 2D turbulence in

Sect. 6.2 and the role of confinement on the dynamics of 2D turbulence in Sect. 6.3. In Sect. 6.4, the main features of the interaction of 2D vortex structures with (no-slip) walls will be discussed. In order to make a connection once again to shallow flows, 2D turbulence experiments in shallow fluids will briefly be reviewed in Sect. 6.5. We conclude with a brief summary of the most important observations in Sect. 6.6.

6.2 Two-Dimensional Turbulence

One of the most striking phenomena of 2D turbulence is the self-organization of the flow. This is clearly visualized in both laboratory experiments in rotating fluids, see Colin de Verdière (1980), Hopfinger et al. (1982), and in stratified fluids, see Boubnov et al. (1994), Yap and Van Atta (1993), Fincham et al. (1996), Maassen et al. (1999), Maassen et al. (2002). It has also been observed in shallow fluid layer and soap film experiments, see Couder (1984), Sommeria (1986), Tabeling et al. (1991), Kellay et al. (1995), Rutgers (1998), Rivera and Ecke (2005, 2016), and Akkermans et al. (2008a), and in many direct numerical simulations of either freely-evolving or forced 2D turbulence. Examples are the studies by McWilliams (1984), Legras et al. (1988), Santangelo et al. (1989), and Boffetta (2007). In the remaining part of this section some of the essential ingredients to understand the dynamics of 2D turbulence will be introduced.

6.2.1 *Inertial Ranges in 2D Turbulence*

One of the most striking differences between 2D and 3D turbulence concerns the weakly dissipative and self-organizing character of 2D turbulent flow compared to the highly dissipative character of 3D turbulence. Consider, for example, a simulation of freely-evolving 2D turbulence, where the flow field is initialized with a random vorticity field; see McWilliams (1984). This initial vorticity field does not contain any coherent vortex structures. During the evolution of the flow field from this initial vorticity distribution, large and approximately axisymmetric vorticity patches emerge as a result of subsequent vortex mergers. The typical lifetime of these vortices turns out to be long compared with the typical flow advection time scale. This self-organization process basically consists of transfer of kinetic energy from the smaller scales of the flow towards larger scales (merging of like-signed vortices) together with vorticity transport to the smaller scales. One can recognize the latter process as the elongation of vorticity filaments in between larger coherent structures. More recently, taking advantage of the increase in computing capabilities, (Boffetta 2007) illustrated this process with an extreme high-resolution simulation of forced 2D turbulence: the flow was forced at some intermediate length scale, and the kinetic energy supplied at the forcing length scale was transported almost completely to the larger and even domain-size scales (a process known as the inverse energy cascade).

Simultaneously, the enstrophy was transported downscale, in what we call the direct enstrophy cascade, to the viscous dissipation range. This is in agreement with the observation by McWilliams (1984) and both cascade ranges were already predicted by Kraichnan (1967, 1971).

From a phenomenological point of view the presence of an inverse energy cascade and a direct enstrophy cascade can be illustrated in the following way. The motion of an incompressible fluid with viscosity ν and density ρ in a plane is described by the 2D velocity field $\mathbf{v}(\mathbf{r}, t) = (u, v)$, with u and v its Cartesian components, and $\mathbf{r} = (x, y)$. The velocity field should satisfy conservation of mass,

$$\nabla \cdot \mathbf{v} = \frac{\partial u}{\partial x} + \frac{\partial v}{\partial y} = 0. \quad (6.1)$$

Conservation of momentum is expressed by

$$\frac{\partial \mathbf{v}}{\partial t} + (\mathbf{v} \cdot \nabla) \mathbf{v} = -\frac{1}{\rho} \nabla p + \nu \nabla^2 \mathbf{v}, \quad (6.2)$$

where we assume that the flow is freely decaying (no injection of energy by external forcing). With the vorticity ω defined as $\omega = \frac{\partial v}{\partial x} - \frac{\partial u}{\partial y}$, we can reformulate Eq. (6.2) into the vorticity equation

$$\frac{\partial \omega}{\partial t} + (\mathbf{v} \cdot \nabla) \omega = \nu \nabla^2 \omega. \quad (6.3)$$

Define the kinetic energy E of the 2D flow as

$$E = \frac{1}{2} \int_{\mathcal{D}} |\mathbf{v}|^2 dA = \int E(k) dk, \quad (6.4)$$

with \mathcal{D} the flow domain of interest, dA an infinitesimal area element of \mathcal{D} , $E(k)$ the energy spectrum and k the wave number. The enstrophy Ω is defined as

$$\Omega = \frac{1}{2} \int_{\mathcal{D}} \omega^2 dA = \int k^2 E(k) dk. \quad (6.5)$$

For the inviscid regime ($\nu = 0$), the kinetic energy is conserved (no dissipation), and the vorticity of a fluid element is also conserved as the vorticity Eq. (6.3) reduces to $\frac{D\omega}{Dt} = \frac{\partial \omega}{\partial t} + (\mathbf{v} \cdot \nabla) \omega = 0$. The latter conservation law also means that any function of the vorticity should be conserved too, thus also the enstrophy must be conserved for inviscid 2D flows. Suppose initially a Gaussian shape of the energy spectrum $E(k)$ which should broaden in time. However, broadening of the energy spectrum $E(k)$ with satisfying both conservation of energy and enstrophy (see Eqs. (6.4) and (6.5)), is only possible when the maximum of the spectrum shifts to lower wave numbers, and energy accumulates in larger-scale structures.

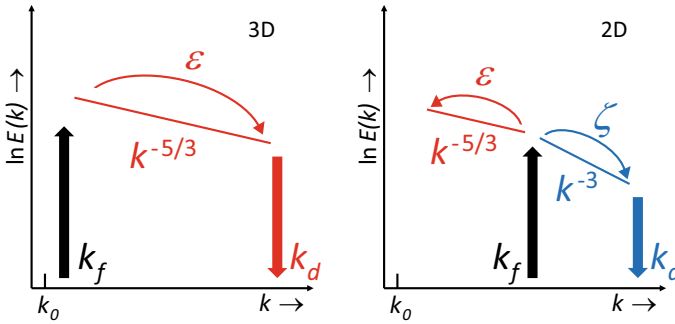


Fig. 6.2 Schematic representation of the inertial ranges in forced 3D turbulence with the direct energy cascade (left), and forced 2D turbulence with both the inverse energy cascade and the direct enstrophy cascade (right). The energy fluxes are denoted by ϵ (to large wave numbers in 3D and small wave numbers in 2D turbulence) and the enstrophy flux is denoted by ζ (to large wave numbers). The forcing wave number k_f is at the largest scales for the 3D case, but at intermediate scales for 2D turbulence; k_d denotes the dissipation wave number

The processes described above are in strong contrast with our experience with cascade processes in homogeneous and isotropic 3D turbulence. In 3D flows, processes like vortex stretching and tilting are present, playing a crucial role in the transfer of kinetic energy from large to small scales in the flow. In 2D flows, these two mechanisms are absent as the vorticity vector is always perpendicular to the plane of flow. In the 3D case, kinetic energy injected at a certain scale (mostly at large scales) is thus transported downscale via the inertial range to the smallest (Kolmogorov) scales where kinetic energy is dissipated.

Summarizing, in 2D turbulence kinetic energy is transported to and collected at the large scales of the flow, the coherent vortex structures. Onsager (1949), Fjørtoft (1953) already predicted on theoretical grounds the emergence of large-scale coherent vortices in 2D flows. In 3D turbulence kinetic energy is transported downscale and is being dissipated, see a schematic sketch of these processes in Fig. 6.2. This difference is responsible for many exciting, and at first sight, somewhat counter-intuitive phenomena that can be observed in large-scale quasi-2D flows.

6.2.2 2D Turbulence: The Early Years

Systematic investigations of homogeneous and isotropic 2D turbulence from a theoretical point of view, and also the first numerical attempts to simulate 2D turbulence, started some 50 years ago by Kraichnan (1967), Leith (1968), and Batchelor (1969). Kraichnan (1967) in his seminal contribution introduced a formal derivation of the scaling of the energy spectrum $E(k)$. He assumed conservation of energy and enstrophy only (in the inviscid limit), and based on that, he proposed for 2D forced turbulence the existence of a dual cascade which are known as the inverse

energy cascade and the direct enstrophy cascade. For the inverse energy cascade, assuming constant energy flux and no enstrophy flux, he found in the inertial range $E(k) \sim \varepsilon^{2/3} k^{-5/3}$. Here, ε is the constant rate of cascade of kinetic energy per unit mass and the expression is valid for $k_L \ll k \ll k_f$ with k_f the wave number at which forcing takes place (injection of energy) and k_L a representative wave number for the large-scale coherent structures. The proposed scaling looks very similar to the Kolmogorov scaling of the energy spectrum in the inertial range of 3D turbulence, but one should realize that the flux in the 3D case is in opposite direction, towards the small dissipative scales. For the inertial range of the direct enstrophy cascade, assuming a constant enstrophy flux and absence of an energy flux, he found a scaling of the spectrum according to $E(k) \sim \zeta^{2/3} k^{-3}$. In this case, ζ is the constant rate of cascade of mean-square vorticity, and the expression is valid for $k_f \ll k \ll k_\zeta$ with k_ζ the enstrophy dissipation scale. See Kraichnan (1971) for a discussion of a logarithmic correction to the energy spectrum in the direct enstrophy cascade range. Numerical simulations of forced 2D turbulence have been carried out since the prediction of the dual cascade, many providing supporting evidence for the dual cascade. As already mentioned before, the extreme high-resolution simulation by Boffetta (2007) has shown convincingly the existence of the dual cascade.

The analysis by Kraichnan (1967) concerned forced 2D turbulence. A few years after Kraichnan's contribution it was (Lilly 1971) who addressed 2D decaying (or freely-developing) turbulence with numerical simulations. One of his motivations was to confirm Kraichnan-Leith-Batchelor (KLB) theory, but also to test Batchelor's results on the time-dependent behavior of the kinetic energy $E(t)$, enstrophy $\Omega(t)$ and the palinstrophy $P(t) = \frac{1}{2} \int_{\mathcal{D}} |\nabla \omega|^2 dA \geq 0$ for decaying flows. From the Navier-Stokes equation for flows with finite viscosity ν one can rather straightforwardly derive the following relations, valid for freely-evolving flows on an unbounded or on a periodic domain:

$$\frac{dE(t)}{dt} = -2\nu\Omega(t) \quad \text{and} \quad \frac{d\Omega(t)}{dt} = -2\nu P(t). \quad (6.6)$$

Since the enstrophy and palinstrophy should always be positive (or zero), we can directly conclude that both the energy $E(t)$ and the enstrophy $\Omega(t)$ should decrease in course of time for decaying 2D turbulence. We can also conjecture that the enstrophy is always bounded by its initial value as $P(t) \geq 0$. In a natural way we then see that $\frac{dE(t)}{dt} \rightarrow 0$ for $\nu \rightarrow 0$. The study by Lilly (1971) indeed confirmed a few results from KLB theory, such as the k^{-3} scaling of the direct enstrophy cascade and the following asymptotic decay relations for $t \rightarrow \infty$ predicted by Batchelor (1969): $E(t) \propto t^{-1}$, $\Omega(t) \propto t^{-2}$, and $P(t) \propto t^{-3}$. However, many numerical studies employing higher resolutions gave deeper insights into both the scaling of the direct enstrophy cascade as the time behavior of energy, enstrophy, and palinstrophy. First of all, in the 1980s quite some evidence emerged about the presence of quite persistent weakly dissipative coherent vortices and the existence of a kind of quasi-steady equilibrium states, see, for example, Fornberg (1977), Matthaeus and Montgomery (1980) and Basdevant et al. (1981), and the already mentioned study

by McWilliams (1984). It was observed that the direct enstrophy cascade occurs as a transient state and often the spectrum steepened considerably, typically showing a k^{-5} scaling behavior (McWilliams 1984; Santangelo et al. 1989). Also a very-high resolution (4096^2 grid points) simulation of decaying 2D turbulence by Bracco et al. (2000) revealed a spectrum with a slope steeper than k^{-3} . Prime suspect of this behavior are the weakly dissipative coherent structures emerging during the decay process (destroying scale invariance); see Santangelo et al. (1989).

6.2.3 Coherent Structures and 2D Turbulence

Keeping the observations with regard to the scaling of the energy spectrum in the enstrophy cascade, and its possible cause, in mind several attempts have been undertaken to analyse theoretically and numerically the temporal evolution of the hierarchy of coherent vortices in such 2D decaying turbulent flows (Carnevale et al. 1991, 1992; Weiss and McWilliams 1993). In the scaling theory proposed by Carnevale et al. (1991), Carnevale et al. (1992) the time evolution of a few quantities have been derived. The vortex density $\rho(t) \propto t^{-\chi}$, the average vortex radius $r(t) \propto t^{-\chi/4}$, the average vortex separation $d(t) \propto t^{-\chi/2}$ and the average enstrophy $\Omega(t) \propto t^{-\chi/2}$, with χ undetermined. With numerical simulations the value $\chi \sim 0.72 - 0.75$ has been found, see Carnevale et al. (1992) and Weiss and McWilliams (1993). With this value it turns out that $\Omega(t) \propto t^{-0.36}$ and $\rho(t) \propto t^{-0.72}$. These scaling relations are remarkably different compared to the predictions by Batchelor (1969) who obtained: $\Omega(t) \propto t^{-2}$ and $\rho(t) \propto t^{-2}$. The high-resolution simulation by Bracco et al. (2000) confirmed the scaling relation for the enstrophy as predicted by the approach of Carnevale and coworkers. They actually found the same exponent for the long-time behavior of the enstrophy: $\Omega(t) \propto t^{-0.36}$. In recent decades many more detailed studies have been reported, see Clercx and Van Heijst (2009) for an overview and references.

From this overview it seems quite evident that the presence of coherent structures in decaying 2D turbulence modifies the KLB-picture. In particular, scaling theories for the vortex population do not support the scaling theory put forward by Batchelor (1969) and the prediction of the scaling of the direct enstrophy cascade in decaying 2D turbulence (in contrast to forced 2D turbulence) is not always confirmed by numerical studies. A final issue concerns the so-called quasi-equilibrium final states. The sea of small-scale vortices will eventually evolve towards a final state by continuous merging processes, see Matthaeus and Montgomery (1980) and McWilliams (1984). Several studies with very-long time integrations have shown that eventually one large-scale dipolar quasi-equilibrium state will emerge (for decaying 2D Navier-Stokes turbulence on a square periodic domain), see Matthaeus et al. (1991).

6.3 2D Turbulence in Square, Rectangular and Circular Domains

Three-dimensional homogeneous and isotropic turbulence is an extremely valuable concept for studies of more general 3D turbulent flows. Although homogeneity and isotropy can be broken by the presence of the boundaries or by the forcing, they are quickly restored when going to smaller length scales. It is this assumption that underlies the Kolmogorov scaling of the energy spectrum in the inertial range. This means that for many fundamental studies, for example on turbulent mixing and inertial particle dispersion on length scales compatible with the inertial range, it may be sufficient to consider the relatively clean case of homogeneous and isotropic 3D turbulence. With the presence of an inverse energy cascade in 2D turbulence, without an energy sink at scales smaller than the domain size, energy is fed into the largest accessible scale. This implies direct interaction of energy-rich eddies with the domain walls, and in the case of no-slip boundary conditions these walls serve as a source of vorticity, even in the freely evolving case (without forcing). This is in strong contrast with 2D freely evolving unbounded (homogeneous and isotropic) turbulence. In that case the enstrophy is necessarily bounded by its initial value, see Batchelor (1969), and no vorticity sources are present.

One of the most striking differences between freely decaying 2D turbulence on a periodic domain and a similar decay process on a 2D confined domain is the shape of the quasi-steady final state. As already mentioned, this quasi-stationary final state on a periodic domain is basically a dipolar vortex, a structure with a patch of positive and a patch of negative vorticity (although under certain conditions exceptions may occur but are quite exceptional). For a square domain with walls, either free-slip (in case of inviscid flows), no-slip or stress-free (the latter two for flows with viscous effects included; the stress-free case will not be discussed here), the quasi-steady final state is different and are generally not a dipolar structure. A variety of statistical-mechanical approaches have been used for the analysis of final states of inviscid flows on confined domains; see Montgomery and Joyce (1974), Pointin and Lundgren (1976), and Chavanis and Sommeria (1996). Typical final states are a monopolar vortex on a square domain (Pointin and Lundgren 1976), a symmetric dipole, an asymmetric dipole or a monopole on a circular domain (depending on the control parameter $\Lambda = \Gamma/\sqrt{2E}$, with Γ the circulation and E the energy; see Chavanis and Sommeria (1996) for details), and a large ellipsoidal or two counter rotating vortices in a rectangular domain with length-to-width ratio of two (with a similar control parameter; see Chavanis and Sommeria (1996)).

6.3.1 Simulations of 2D Turbulence in Domains with No-Slip Walls

From now on, we will consider decaying 2D Navier-Stokes turbulence on confined domains with no-slip walls, which was the natural next step towards flows with realistic boundary conditions and, moreover, experimentally accessible flow configurations (Li and Montgomery 1996; Li et al. 1997; Maassen et al. 1999, 2002, 2003; Clercx et al. 1998, 1999, 2001; Schneider and Farge 2005, 2008; Keetels et al. 2010; Fang and Ouellette 2017).

We first focus on the quasi-steady final states. Here, some care is needed as the final state is always cessation of any flow. However, at an earlier stage during the decay process small-scale features are dissolved due to merging processes and sometimes disappear due to viscous dissipation. At a later stage, one final structure remains and is rather persistent for a very long time. This is what we call the quasi-steady final state. Some observations from both laboratory experiments of decaying quasi-2D turbulence in stratified fluids (Maassen et al. 1999, 2002, 2003) and direct numerical simulations (Clercx et al. 1998, 1999, 2001) with regard to the so-called quasi-steady final states are the following. In square containers, we found mostly a monopolar final state, and when the initial flow was more energetic, a tripolar state is found. The latter state is basically the result of the interaction of a rapidly rotating monopolar vortex that generates strong boundary layers at the no-slip wall. These boundary layers detach, roll up and form the satellite vortices. The minority of the end states in the numerical simulations had a dipolar-like character. Maybe the most remarkable result has been the phenomenon of spontaneous spin-up of the flow that initially had no angular momentum (Clercx et al. 1998). The higher the Reynolds number the more likely is spin-up to occur, with about 50% of the runs having a final state with clockwise rotation and the rest having counter-clockwise rotation (Keetels et al. 2010).

Spontaneous spin-up can be quantified by measuring the time evolution of the angular momentum $L(t)$ contained by the flow. The angular momentum is defined as

$$L(t) = \int_{\mathcal{D}} \hat{\mathbf{z}} \cdot (\mathbf{r} \times \mathbf{v}(\mathbf{r}, t)) dA, \quad (6.7)$$

with $\hat{\mathbf{z}}$ the unit vector normal to the plane of flow, the origin of the coordinate system (x, y) in the center of the container, and \mathbf{r} the position vector. In the numerical experiments mentioned above, the angular momentum at $t = 0$ was negligible, $L(t = 0) = L_0 = 0$. The rate of change of angular momentum can straightforwardly be determined by taking the time derivative of Eq. (6.7) and substituting the Navier-Stokes Eq. (6.2) into the resulting expression for $\frac{dL}{dt}$. It yields the following integral (in dimensionless form) over the boundary $\partial\mathcal{D}$ of the domain,

$$\frac{dL}{dt} = \int_{\partial\mathcal{D}} p(\mathbf{r}, t) \mathbf{r} \cdot d\mathbf{s} + \frac{1}{\text{Re}} \int_{\partial\mathcal{D}} \boldsymbol{\omega}(\mathbf{r}, t) (\mathbf{r} \cdot \hat{\mathbf{n}}) ds. \quad (6.8)$$

Here, $\hat{\mathbf{n}}$ is a unit vector normal to the boundary, $d\mathbf{s}$ is an infinitesimal boundary element (tangential to the boundary) and ds its magnitude. This relation clearly shows that angular momentum production is due to a pressure contribution (inviscid) and a viscous contribution proportional to the vorticity generated at the boundary. The pressure contribution turns out to be the dominant term in the range of Reynolds numbers considered in the experiments and simulations. More extensive discussions on this phenomenon can be found in (Clercx et al. 1998; Clercx and Van Heijst 2009; Keetels et al. 2010).

In the experiments mentioned above and in most of the numerical studies, the integral scale Reynolds number $Re = U_{rms}L/\nu$ (based on the initial root-mean-square velocity U_{rms} , the size of the container L , and the fluid kinematic viscosity ν) is relatively low. In the experiments, $1000 \lesssim Re \lesssim 2000$, and in the numerical simulations, we typically have $1000 \lesssim Re \lesssim 5000$, with a very few cases with $Re = 10^4$ or 2×10^4 . The more recent numerical simulations by Keetels et al. (2010) were carried out with significantly higher initial large-scale Reynolds number, up to $Re = 10^5$. In Fig. 6.3, we show a typical evolution of decaying 2D turbulence on a square domain with no-slip rigid walls. The initial flow field consisted of an almost regular array of 10×10 Gaussian vortices. The positions of these vortices are all slightly disturbed to give the evolution a kick-start towards a fully turbulent flow. The quasi-steady final state that emerges after about 400 initial eddy turnover times is basically a relatively strong, but also relatively small monopolar vortex embedded in a large-scale swirling flow. Also several smaller vortices are embedded in this swirling background flow, and these vortices are mostly the result of detachment and roll up of boundary layers containing high-amplitude vorticity.

During the decay process the impact of the no-slip walls is large: many relatively small or even tiny vortices can be observed in each of the panels of Fig. 6.3. These small vortices are almost all generated at the no-slip walls, signifying a crucial difference between 2D decaying spatially unbounded turbulence and 2D decaying confined turbulence. It affects the vortex statistics, which is discussed in more detail in (Clercx and Van Heijst 2009), and also the enstrophy production and decay rate significantly. To illustrate the different decay scenarios, we show in Fig. 6.4 two snapshots from simulations starting with exactly the same initial conditions. The left panel shows the result with no-slip walls and the right panel those with periodic boundary conditions (Keetels et al. 2010).

6.3.2 *Quasi-Steady Final States: Laboratory Experiments*

Quasi-steady final states can also be explored in laboratory experiments. Here, and as a typical illustration, the decay scenarios of quasi-2D turbulence in laboratory experiments, carried out in a two-layer stratified fluid in circular containers (for experimental details, see Maassen et al. (1999)), are briefly discussed. See also Yap and Van Atta (1993) and Fincham et al. (1996) for similar experiments a few years earlier. Two sets of experiments in cylindrical containers have been carried out by

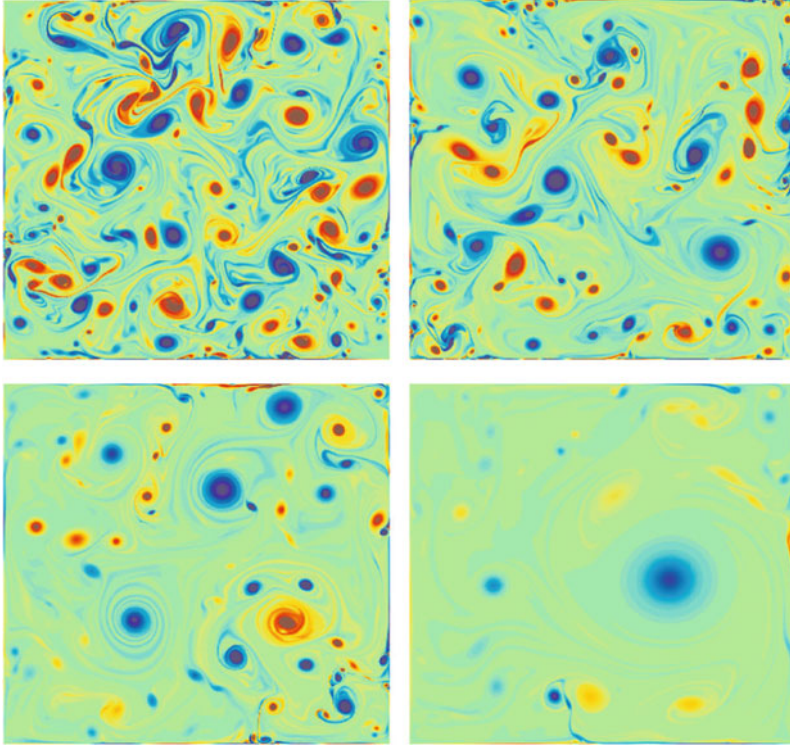


Fig. 6.3 A few vorticity snapshots showing the process of spontaneous spin-up. The Reynolds number of the simulation is $Re = 5 \times 10^4$. The snapshots are taken at $\tau = 8, 24, 100$ and 400 eddy turnover times (with $\tau = 1$ corresponding to the initial eddy turnover of the initial vortices). The initial flow field consisted of an array of 10×10 vortices with positions slightly distorted to enhance the rapid evolution towards an irregular turbulent flow field. For computational details, see Keetels et al. (2010)

Maassen and collaborators, all in the spirit of (Li and Montgomery 1996; Chavanis and Sommeria 1996): a set with initially hardly any swirl ($L_0 \approx 0$) and a set with an initial condition with considerable swirl ($L_0 \neq 0$). The initial flow was generated by dragging a rake through the stratified fluid. At a large enough towing speed the wake behind each bar becomes turbulent, thus generating a turbulent initial flow field. Symmetric rakes result in $L_0 \approx 0$, and asymmetric rakes result in $L_0 \neq 0$, see Maassen et al. (1999) for details. The Reynolds number of the (initial) flow, now defined as $Re = U_{rms} R / \nu$ with R the radius of the container, is $Re \approx 4000$. The experiments with $L_0 \approx 0$ show the classical decay process. The small vortices, generated by initializing the flow, start the merge quickly with like-sign counterparts and the flow evolves towards a quadrupolar state. This evolution is due to a permanent interaction of the flow with the rigid circular no-slip walls. Finally, a more or less quasi-steady dipolar final state appears. The other set of experiments, with $L_0 \neq$

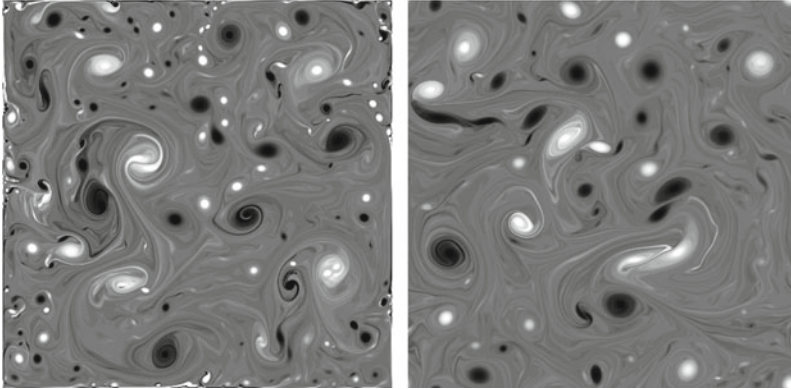


Fig. 6.4 Vorticity snapshots, taken at dimensionless time $\tau = 15$, from a simulation with no-slip rigid walls (left panel) and a simulation with periodic boundary conditions (right panel). The initial conditions were exactly the same for both numerical experiments and in both cases: $Re = 10^5$. Dark and light grey represent positive and negative vorticity, respectively. Courtesy Keetels et al. (2010)

0, show basically a similar initial decay stage, but due to the swirl, a large-scale monopolar vortex forms instead of a quadrupolar or dipolar state. This monopolar vortex easily slides along the circular rigid walls, and less boundary-layer vorticity is produced in this case (compared to the square container). The experimental results are in very good agreement with the numerical simulations by Li et al. (1997). The experimentally observed quasi-steady states agree remarkably well with the predictions by Chavanis and Sommeria (1996) for inviscid flows in confined domains: a dipole when initially the circulation is zero, and a monopole when the initial condition contains circulation.

These experiments of decaying 2D turbulence in circular domains show that for $L_0 \approx 0$ the quasi-steady final state is a quadrupolar or dipolar structure, thus no spontaneous spin-up. Absence of spontaneous spin-up on circular domains was confirmed later on in numerical studies by Schneider and Farge (2005). This can be understood using Eq. (6.8). In circular domains, the pressure contribution to the production of angular momentum vanishes as $(\mathbf{r} \cdot \hat{\mathbf{n}}) = 0$, thus the dominant term vanishes for this particular geometry. The domain shape is thus relevant in determining the quasi-steady final state by flow-wall interaction.

In a similar spirit, laboratory experiments in two-layer density stratified fluids and numerical simulations have been carried out to explore the quasi-steady final states of 2D decaying turbulence in rectangular containers with aspect ratios $\delta = L/W$, with L the length and W the width of the container, varying from $\delta = 2$ to $\delta = 5$ (Maassen et al. 2003). The number of vortices N_f in the final quasi-steady cell pattern is in most experiments either $N_f = \delta$ or $N_f = \delta \pm 1$. This is not fully surprising, and is consistent with observations as shown in Fig. 6.1 for the gyres in the Gulf of Aden and the number of vortices observed in the Adriatic Sea. Another observation concerned the comparison of the present results, for the case $\delta = 2$, with results

of the quasi-steady final states in inviscid flows in domains with the same aspect ratio; see Pointin and Lundgren (1976) and Chavanis and Sommeria (1996). A clear discrepancy was reported which most likely is due to the role of the boundary layers present in the experiments but absent in the case of inviscid flows.

6.3.3 *Forced 2D Turbulence on Confined Domains*

The discussion above focuses solely on decaying 2D turbulence. However, the formation of domain-size monopolar vortices has also been observed in forced 2D turbulence in square domains. Both in experiments, see Sommeria (1986) and Paret and Tabeling (1998), and in numerical studies, see Molenaar et al. (2004) and Van Heijst et al. (2006). In particular the experimental study by Sommeria (1986) and numerical results reported by Van Heijst et al. (2006) revealed reversals of the swirl of the large-scale monopolar vortex. The time between reversals is orders of magnitude longer than the time scale needed for a reversal to occur, which is of the order of a few large-scale eddy turnover times. The initialization of these reversals was attributed to destabilizing disturbances such as small strong eddies (Sommeria 1986) but their origin was not entirely clear. In numerical studies of forced 2D turbulence in square domains with rigid no-slip sidewalls, with similar forcing length scale as the experiments by Sommeria, it became clear that the disturbances originate from formation and detachment of the boundary layers at the sidewall and subsequent roll up of the boundary-layer filaments into small strong vortices (Van Heijst et al. 2006). When strong enough, they may destabilize and potentially disintegrate the large-scale monopolar vortex. A new large-scale vortex will quickly build up after this event, with same or opposite rotation sense. As an illustration of this process three consecutive snapshots of the vorticity field from a forced 2D turbulence simulation in a square confined domain with no-slip sidewalls, provided by Molenaar et al. (2004), are shown in Fig. 6.5. The integral-scale Reynolds number of this simulation was approximately 3000. The snapshots are taken just before the collapse, during the collapse stage and just after it, when once again a domain-filling monopolar vortex has formed (with opposite sign vorticity in this case). The lower panel shows the normalized angular momentum computed according to Eq. (6.7) of the same run. It clearly shows the existence of domain-filling monopolar vortices over many turnover times and the collapse stages of relative short duration. Note that the vorticity snapshots in Fig. 6.5 are taken at $t = 800, 900$ and 1000 , respectively. This kind of phenomena is a clear manifestation of the impact of rigid no-slip sidewalls on the dynamics of 2D turbulence.

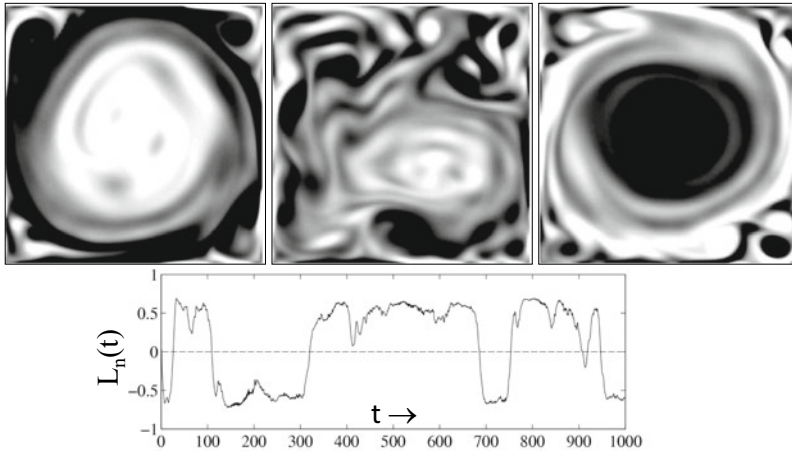


Fig. 6.5 Snapshots of the vorticity evolution from a forced 2D turbulence simulation in a square domain with no-slip walls. The snapshots are taken just before (left panel, $t = 800$) and just after (right panel, $t = 1000$) the sign reversal of a large monopolar vortex. The panel in the middle ($t = 900$) is taken during the collapse stage. Large negative values of vorticity are indicated with black, and white indicates large positive values of vorticity. The lower panel shows the normalized angular momentum of the flow in the square box, showing distinct phases of spin-up with collapse stages in between. Normalization is done with the angular momentum of uniform rotation with the same energy content $E(t)$ as the actual flow field. Courtesy Molenaar et al. (2004)

6.4 Interaction of Vortices with Walls

In the previous section, we have discussed the large-scale flow structures emerging during the decay of 2D turbulence in confined domains. There was a clear impact of the presence of rigid walls and the domain geometry on the quasi-stationary final states. However, we could also observe during the decay process the formation of many small-scale vortices containing high values of vorticity; see Figs. 6.3 and 6.4. The production of these small-scale vortices by detaching boundary layers also has a strong impact on the vortex statistics and the time evolution of the vortex density, vortex separation and the enstrophy is strongly affected when rigid no-slip walls are present. See for a further discussion of this particular aspect (Clercx and Van Heijst 2009). Such small-scale vortices might also be the cause of reversals of large-scale vortical structures in 2D forced turbulence in confined domains.

6.4.1 No-Slip Walls as Vorticity Sources

The formation of small-scale vortices near rigid no-slip walls indicate that flow-wall interactions are relevant for 2D turbulence in confined domains. It is expected that the larger and stronger the vortices, the larger their impact on the evolution of 2D

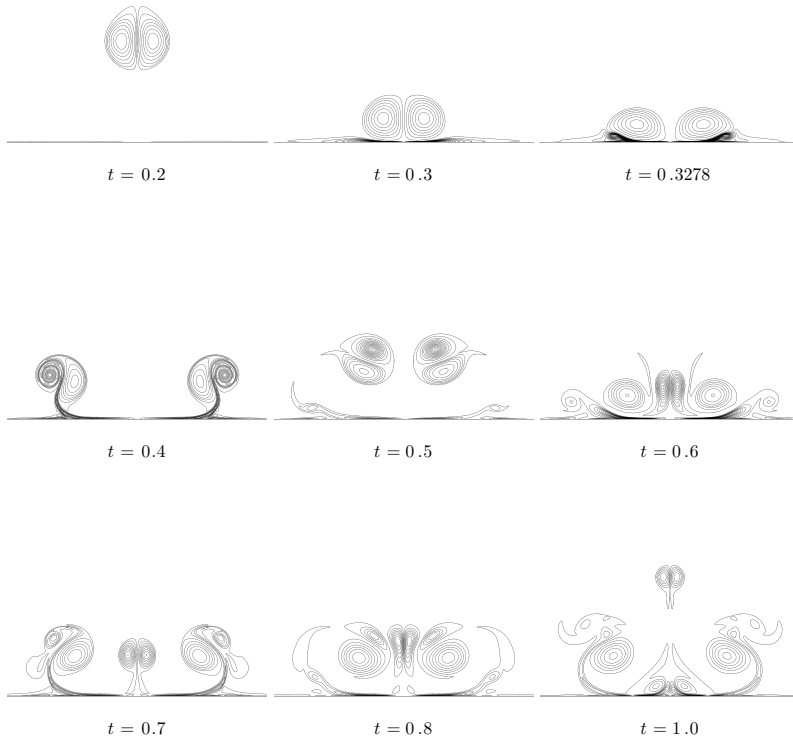


Fig. 6.6 Sequence of vorticity contour plots showing the flow evolution of a dipole-like vortex colliding with a rigid no-slip wall. The integral-scale Reynolds number, based on the initial speed and radius of the dipole, is $Re = 2500$. Courtesy Kramer et al. (2007)

turbulence. This is, in particular, due to the production of more intense boundary layers, that once again detach and create new strong vortices that travel to the interior. In other words, the rigid walls serve as a source of enstrophy, and this also implies enhanced dissipation of kinetic energy. One of the open questions here is what happens in the limit of vanishing viscosity, or in other words: what will happen when $Re \rightarrow \infty$? Will there be a finite dissipation in the inviscid limit for 2D flows in confined geometries?

A variety of approaches can be used to tackle this problem. One of these is the dipole-wall collision experiment, see Fig. 6.6, which has recently been reviewed by Clercx and Van Heijst (2017). In particular, one can explore how vorticity production during a vortex-wall collision is enhanced and how this affects the dissipation of kinetic energy. For this purpose we need to introduce a slightly revised version of the evolution equation of the enstrophy, which was introduced in Sect. 6.2 for the unbounded or periodic domain. For domains bounded with no-slip walls we need to add an additional term, a boundary integral, yielding

$$\frac{d\Omega(t)}{dt} = -\frac{2}{\text{Re}}P(t) + \frac{1}{\text{Re}} \int_{\partial\mathcal{D}} \omega \frac{\partial\omega}{\partial n} ds, \quad (6.9)$$

with $\frac{\partial}{\partial n}$ the wall-normal derivative and ds an infinitesimal element of the boundary $\partial\mathcal{D}$. The time rate of change of the enstrophy is expressed in dimensionless form. The boundary integral may substantially increase the enstrophy at some instants of time, in such a way, that as a net effect, enstrophy is produced during vortex-wall collisions. Although the time rate of change of the kinetic energy will keep the same form, here in dimensionless quantities written as

$$\frac{dE(t)}{dt} = -\frac{2}{\text{Re}}\Omega(t), \quad (6.10)$$

the persistence of enstrophy, or even the increase of enstrophy, will automatically imply stronger decay of the kinetic energy of the flow. Note that for 2D decaying flows on periodic domains the enstrophy is always bounded by its initial value (Batchelor 1969), thus the dissipation will reduce to zero in the inviscid limit, or: $\frac{dE(t)}{dt} \propto \text{Re}^{-1} \rightarrow 0$ for $\text{Re} \rightarrow \infty$. The question to be answered is whether the enstrophy production scales with the Reynolds number, which might be expected as the boundary layers generated during the vigorous vortex-wall collisions contains large amount of vorticity. Suppose that $\Omega \propto \text{Re}^\alpha$ for $\text{Re} \rightarrow \infty$. This would imply

$$\frac{dE}{dt} = -\frac{2}{\text{Re}}\Omega \propto \text{Re}^{\alpha-1}. \quad (6.11)$$

Obviously, when the enstrophy does not scale with the Reynolds number, or $\alpha = 0$, the original result is retrieved: $\frac{dE}{dt} \rightarrow 0$ when $\text{Re} \rightarrow \infty$. In the case that $\alpha = 1$, or $\Omega \propto \text{Re}$ for $\text{Re} \rightarrow \infty$, we end up with constant energy dissipation in the inviscid limit, reminiscent to 3D turbulence. Some recent works have indeed indicated that $\alpha \neq 0$, but debate exists about its precise value and its potential implications; see Clercx and Van Heijst (2002, 2017), Sutherland et al. (2013), and Nguyen van yen et al. (2011, 2018), and values for α are found in the range 0.5–1.0.

6.4.2 Vorticity Production by Dipole-Wall Collisions

Exploration of vorticity production at walls is based on numerical experiments of dipole-wall collisions with a rigid flat wall (with no-slip boundary conditions), as for the first time investigated by Orlandi (1990). The original motivation of this kind of studies were related to the problem of trailing vortices from aircraft, which will interact with the ground during landing and take-off resulting in vortex rebounds. Later on, the mechanism for inviscid dipole-vortex rebounds became also a topic of interest in the geophysical flow community. There, vorticity production by stretching of vortex tubes in the presence of a sloping bottom in the coastal zone could be

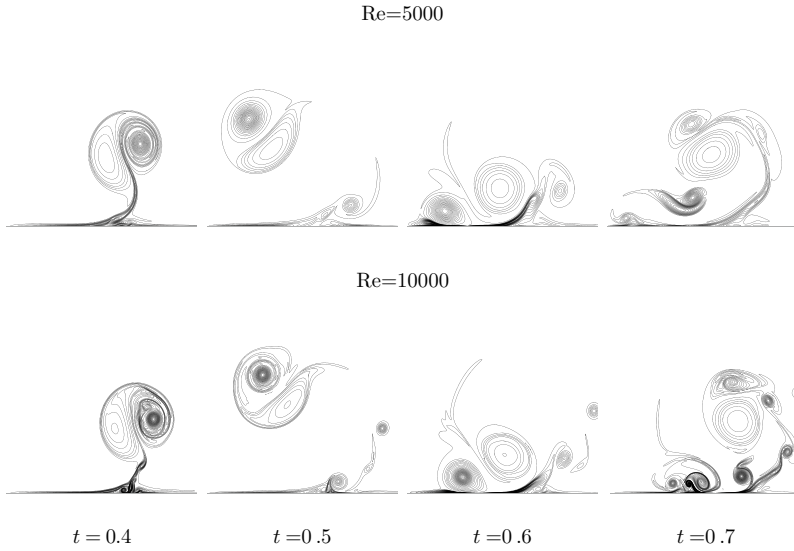


Fig. 6.7 Sequence of vorticity contour plots illustrating the flow evolution during a dipole-wall collision for $\text{Re} = 5 \times 10^3$ (top panel) and $\text{Re} = 10^4$ (bottom panel). The plots only show the right-hand side part of the domain as the dipole-wall collision is symmetric with regard to the dipole axis, see also Fig. 6.6. Courtesy Kramer et al. (2007)

used to parameterize aspects of 3D vortex dynamics for a 2D description of the inviscid rebound process (Carnevale et al. 1997). The complexity of dipole-wall collisions, with vortex rebounds already for relatively low Reynolds numbers, is nicely illustrated in Fig. 6.7. A brief review with regard to dipole-wall collisions is provided by Clercx and Van Heijst (2017).

First numerical observations of Reynolds-number dependency of enstrophy production during dipole-wall collisions were reported by Clercx and Van Heijst (2002). They revealed that $\Omega \propto \text{Re}^{0.8}$ for $\text{Re} \lesssim 2 \times 10^4$ and $\Omega \propto \text{Re}^{0.5}$ for $\text{Re} \gtrsim 2 \times 10^4$, with the Reynolds number based on the radius of the dipole R_d , and its self-induced traveling speed U_d . The scaling of the enstrophy implies $\frac{dE}{dt} \propto \text{Re}^{-0.2}$ and $\frac{dE}{dt} \propto \text{Re}^{-0.5}$ for the respective regimes. This scaling behavior turned out to be independent of the collision angle of the dipole with the rigid wall. A simple scaling analysis for the large-Reynolds number regime (where $\Omega \propto \text{Re}^{0.5}$) is based on the following balance at the flat rigid wall (chosen parallel with the x – axis of a reference frame),

$$-v \frac{\partial \omega}{\partial y} \Big|_{\text{wall}} = \frac{1}{\rho} \frac{\partial p}{\partial x} \Big|_{\text{wall}}, \quad (6.12)$$

which can directly be obtained from the Navier-Stokes equation. In the following, we assume that the boundary layer remains laminar (but unsteady), an assumption that eventually may break down at much higher Reynolds number values. When we

assume that the pressure distribution along the boundary is finite, we may immediately conclude from Eq. (6.12) that $\frac{\partial \omega}{\partial y}|_{\text{wall}} = \mathcal{O}(\text{Re})$ for large Reynolds number values. The boundary-layer thickness δ scales according to Prandtl's prediction: $\delta \propto \text{Re}^{-1/2}$. This immediately implies, using the predicted scaling of the vorticity gradient normal to the wall, that $\omega|_{\text{wall}} \propto \sqrt{\text{Re}}$. Provided that the Reynolds number is large enough (here $\text{Re} \geq 2 \times 10^4$), we can expect that the total enstrophy and palinstrophy in the flow will be dominated by the vorticity and vorticity gradient values in the boundary layer itself. We can then easily derive the following estimates: $\Omega \propto R_d \delta \omega^2|_{\text{wall}} \sim R_d \sqrt{\text{Re}}$. For the palinstrophy we can derive in a similar way: $P \propto R_d \delta (\frac{\partial \omega}{\partial y})^2|_{\text{wall}} \sim R_d \text{Re} \sqrt{\text{Re}}$. This is consistent with the scaling of the palinstrophy reported by Clercx and Van Heijst (2002): $P \propto \text{Re}^{1.5}$ for $\text{Re} \gtrsim 2 \times 10^4$ and $P \propto \text{Re}^{2.25}$ for $\text{Re} \lesssim 2 \times 10^4$. It is interesting to note that a scaling analysis for $\text{Re} \lesssim 10^4$ by Keetels et al. (2011) provided similar scaling exponents, $\Omega \propto \text{Re}^{3/4}$ and $P \propto \text{Re}^{9/4}$ (compared to $\text{Re}^{0.8}$ and $\text{Re}^{2.25}$, respectively, found by Clercx and Van Heijst (2002)).

In recent years, a few more studies emerged addressing the possible existence of extremely thin dissipation layers near the rigid wall, including the possible presence of a slip-velocity at the rigid wall (Nguyen van yen et al. 2011, 2018; Sutherland et al. 2013). Nguyen van yen et al. (2011) did a first attempt, based on a similar dipole-wall collision experiment as discussed above, to explore a possible Re-independent energy dissipation rate. In other words, they explored the possibility of the existence of $\frac{dE}{dt} \rightarrow \chi$ for $\text{Re} \rightarrow \infty$ with $\chi < 0$ and constant. Such behavior would be in sharp contrast with the standard result for 2D decaying turbulence in unbounded (or periodic) domains. In their analysis they complemented Prandtl's boundary layer argument with some theorems put forward by Kato (1984) on the dissipation rate in the vanishing viscosity limit and showed two scaling regimes for the enstrophy. For the early stage and initial collision stage they found $\Omega \propto \text{Re}^{0.5}$ and during the collision stage (and boundary-layer detachment) they found $\Omega \propto \text{Re}$. The latter regime implies indeed finite kinetic energy dissipation at ever larger Reynolds numbers. These results were subsequently critically examined by Sutherland et al. (2013) who provided supporting evidence of the earlier predicted scaling relation: $\frac{dE}{dt} \propto \text{Re}^{-0.5}$. We should however emphasize that the studies by Nguyen van yen et al. (2011) and Sutherland et al. (2013) do not actually extend the range of Reynolds numbers compared to (Clercx and Van Heijst 2002; Keetels et al. 2011). Therefore, we should still be careful to come to strong conclusions applicable for the vanishing viscosity limit.

The discussion on the dissipation rate in the vanishing viscosity limit is still ongoing; see Nguyen van yen et al. (2018). Moreover, the analysis presented so far are based on laminar Prandtl boundary layer theory and possible implications of boundary-layer detachment, but no deeper analysis is available for the case the boundary layers become fully turbulent, a scenario that is expected to become important when Re is further increased.

6.5 Review of 2D Turbulence Experiments in Shallow Fluids

In environmental flows, such as in estuaries and rivers (Uijttewaal 2014), suppression of vertical motion and subsequent quasi-two-dimensionalization occurs predominantly by the shallowness of the flow domain. Planetary rotation is almost irrelevant on these scales and density stratification is mostly not important (but not excluded in certain cases). For this reason shallow flow experiments have been used to study aspects of quasi-2D turbulence (Chen and Jirka 1995; Uijttewaal and Jirka 2003) and dynamics of coherent structures in shallow flows, including secondary out-of-plane motion (Jirka 2001; Lin et al. 2003; Sous et al. 2004, 2005; Akkermans et al. 2008a, 2010; Kelley and Ouellette 2011; Duran-Matute et al. 2010, 2011; Tithof et al. 2018).

This overview of shallow fluid layer experiments will focus on the larger scale flow phenomena such as the dynamics of vortices, the evolution of global integral quantities like energy and enstrophy, and the eventual presence of 3D secondary flows. Quasi-steady final states belong to this class of phenomena but have already been discussed in Sect. 6.3. For an extensive discussion of the statistical properties of the velocity and vorticity field and the Lagrangian dispersion of tracers, also experimentally explored by means of shallow fluid layer and soap film experiments, the reviews by Tabeling (2002), Kellay and Goldburg (2002), Clercx and Van Heijst (2009), and Boffetta and Ecke (2012) can be consulted.

In the preceding section, we have discussed the implications of the lateral boundaries in 2D confined turbulence and their impact on a variety of physical processes, including coherent structure formation, vorticity production at rigid walls, and dissipation of kinetic energy. Shallow flows, both in geophysical systems and in laboratory experiments, need to be supported by a bottom, which implies an additional damping mechanism affecting the flow, thus an additional source of dissipation. Furthermore, the bottom will contribute to the emergence of 3D secondary flows. This damping mechanism and the weak 3D recirculation flows in these systems, are not represented in 2D (confined) turbulence. Their impact needs to be known for better understanding of the quasi-2D behavior of environmental and geophysical flows.

Since the mid-1980s the first experiments have been reported addressing a variety of aspects of 2D turbulence. In particular, several of the exciting theoretical and numerical findings based on KLB theory were put to a test, such as the inverse energy and direct enstrophy cascade, the associated energy and enstrophy fluxes, statistical quantities with regard to the fluctuating velocity and vorticity fields, vortex statistics of freely evolving 2D turbulence, Lagrangian dispersion properties of passive tracers (including pair dispersion), and last but not least, the emergence of so-called condensation phenomena (Smith and Yakhot 1993). The last phenomenon is a clear result of the inverse energy cascade as energy injected at some intermediate scale is transferred upwards to the largest scales, and eventually this inverse cascade is arrested by the finiteness of the container, a manifestation of confinement (see also the brief discussion in the last paragraph of Sect. 6.3).

Laboratory experiments can be carried out with a variety of generation mechanisms for quasi-2D flows. One could think of rapidly rotating homogeneous fluids, see, for example, the pioneering works by Colin de Verdière (1980) and Hopfinger et al. (1982), or in homogeneous density-stratified (or two-layer) fluids, see, for example, Yap and Van Atta (1993), Boubnov et al. (1994), Fincham et al. (1996), and Maassen et al. (1999). We will not further discuss this kind of experiments (but see Sect. 6.3 for some results on quasi-steady final states). We will focus on a discussion of experiments in shallow fluid layers where two-dimensionality is enforced by geometrical confinement only (and this will mostly exclude soap film experiments for which the interested reader is referred to Kellay and Goldburg (2002)).

6.5.1 *Laboratory Experiments in Shallow Fluid Layers*

The first shallow flow experiment aimed at verifying aspects of KLB-theory was reported by Sommeria (1986). His experiments were mostly focused on the measurement of the 2D inverse energy cascade which he was able to confirm. For this purpose he generated 2D turbulence in a shallow layer of mercury. By applying a uniform magnetic field (with the field lines perpendicular to the shallow mercury layer) 3D motions could be strongly suppressed. This approach resulted in a pretty horizontal velocity field in a substantial part of the mercury layer. Near the bottom plate a very thin viscous boundary layer is present which affects the flow in the core in the form of a linear damping, i.e. proportional to the local horizontal fluid velocity in the core. Larger coherent structures have larger velocities, and linear damping particularly affects these larger scales and potentially can serve as a sink of energy to arrest the inverse energy cascade at a certain scale.

As mercury has certain serious disadvantages, such as being inaccessible for optical diagnostics to measure the fluid velocity inside the fluid layer, but also its toxic properties (thus requiring quite some precautions to work safely) a different kind of experiment was necessary. A new setup was proposed not many years later by Tabeling et al. (1991) and Dolzhanskii et al. (1992), which initiated many laboratory investigations on 2D turbulence worldwide. These experiments have been carried out in a shallow layer of electrolyte and the forcing mechanism is based on the interaction of a current density with a magnetic field inducing the Lorentz force driving the fluid motion. For this purpose magnets are placed underneath the fluid layer and two electrodes are placed on opposite sides of the container providing a uniform electrical current that runs through the electrolyte to effectively force the fluid motion. To achieve quasi-2D flow the horizontal scale of motion L must be much larger than the fluid-layer thickness H . Under these conditions, it is usually assumed that due to mass conservation $w \approx (H/L)U$, with w and U the vertical and horizontal velocity scale, respectively. At first sight, the two-dimensionality of the flow can thus be tuned with the magnet size and fluid-layer thickness.

An important test for the shallow fluid layer setup was the comparison of experimentally obtained vortex statistics data with theoretical and numerical results

by Carnevale et al. (1991, 1992). Cardoso et al. (1994) found $\rho(t) \propto t^\chi$ with $\chi = 0.44 \pm 0.1$, quite different compared to the value reported by Carnevale and coworkers: $\chi \approx 0.72 - 0.75$. They also did not observe a rapid decrease of the area occupied by the vortices as expected from the approach by Carnevale and coworkers. Besides the fact that the integral-scale Reynolds number was of the order 1000–2000, so that the flow is affected by viscous dissipation, bottom friction could explain this deviation. Later, Akkermans et al. 2008b,a identified significant 3D recirculating flows in shallow fluid layers uncovered by stereo-PIV measurements (and confirmed in simulations) as another potential reason for deviations. Thus vertical confinement and bottom friction might complicate the picture considerably.

6.5.2 2D Turbulence with Rayleigh Friction

For the analysis of bottom friction it is often assumed that the vertical profile of the horizontal motion can be approximated by a Poiseuille profile (satisfying the boundary conditions at the no-slip bottom and stress-free surface). This allows us to reformulate the Navier Stokes Eq. (6.2) by replacing the viscous contribution $\nu(\partial^2 \mathbf{v} / \partial z^2)$ by the term $-\lambda \mathbf{v}$. This linear damping term is known as Rayleigh friction and the bottom or Rayleigh friction coefficient takes the form $\lambda = \nu(\frac{\pi}{2H})^2$. We can now parameterize the quasi-2D flow in shallow fluid layers by the following dimensionless equation:

$$\frac{\partial \mathbf{v}}{\partial t} + (\mathbf{v} \cdot \nabla) \mathbf{v} = -\nabla p + \frac{1}{\text{Re}} \nabla^2 \mathbf{v} - \frac{1}{\text{Re}_\lambda} \mathbf{v} + \mathbf{F}_L, \quad (6.13)$$

with \mathbf{v} representing the horizontal flow field only, satisfying 2D mass conservation, Re_λ the ratio of the bottom-friction time scale and the large-scale eddy turnover time scale of the horizontal flow, and \mathbf{F}_L the Lorentz force to drive the flow. In these shallow electrolyte solutions the typical integral scale Reynolds number is about 1000–2000.

Taking into account the presence of bottom friction an upgrade of this kind of experiments has been proposed few years later to suppress the effects of bottom friction (Marteau et al. 1995; Hansen et al. 1998). The new experiments consist of two thin layers of electrolyte on top of each other, the bottom layer heavier than the top layer, to reduce the impact of bottom friction (and to suppress vertical velocities). The flow is only effectively forced (in a similar way as described above) in the bottom layer. Coupling with the top layer occurs via the stress boundary condition at their interface. They repeated the experiments by Cardoso et al. (1994) and found the encouraging result $\chi \approx 0.70 \pm 0.1$. The observed decay scenario of the 2D turbulent flow was quite similar as in the 2D simulations (with similar integral-scale Reynolds number) reported by Clercx et al. (1999) and Wells and Afanasyev (2004). Moreover, their vortex statistics scenario turned out to be quite similar to those observed by Clercx and Nielsen (2000) and Clercx et al. (2003) for decaying

2D turbulence in confined domains. These shallow fluid experiments provide strong evidence that 2D turbulence decay scenarios follow those of 2D decaying and confined turbulence and not the vortex statistics scenario by Carnevale and coworkers. Quite remarkable, a similar stereo-PIV analysis by Akkermans et al. (2010) revealed that also in stratified two-layer shallow flows 3D recirculating flows of similar magnitude as in the single-layer experiments occur, implying that the two-layer solution is not extremely effective in suppressing vertical velocities. This puts into question the quasi-two-dimensionality of such flows. Although all these results are valuable for understanding quasi-2D turbulence, any interpretation of experimental data is still a delicate issue and should be done with care.

As laboratory experiments and confined 2D turbulence simulations appear to provide similar decay scenarios it might be helpful to have a closer look at decaying 2D flow with Rayleigh friction. The discussion below is based on Eq. (6.13) without forcing term. The dimensionless 2D vorticity equation is then

$$\frac{\partial \omega}{\partial t} + (\mathbf{v} \cdot \nabla) \omega = \frac{1}{\text{Re}} \nabla^2 \omega - \frac{1}{\text{Re}_\lambda} \omega. \quad (6.14)$$

With the definitions of the kinetic energy and enstrophy of the flow, see Eqs. (6.4) and (6.5), we can derive the following expression for the time rate of change of the kinetic energy

$$\frac{dE(t)}{dt} = -\frac{2}{\text{Re}} \Omega(t) - \frac{2}{\text{Re}_\lambda} E(t). \quad (6.15)$$

By separating Rayleigh friction from ordinary 2D flow dynamics the energy is written as $E(t) = E_0(t)e^{-2t/\text{Re}_\lambda}$ and the enstrophy as $\Omega(t) = \Omega_0(t)e^{-2t/\text{Re}_\lambda}$, with $E_0(t)$ and $\Omega_0(t)$ the compensated energy and the enstrophy, respectively, we simplify Eq. (6.15) to

$$\frac{dE_0(t)}{dt} = -\frac{2}{\text{Re}} \Omega_0(t). \quad (6.16)$$

This suggests that the 2D velocity field and the vorticity field can be written as $\mathbf{v}(\mathbf{r}, t) = \mathbf{v}_0(\mathbf{r}, t)e^{-t/\text{Re}_\lambda}$ and $\omega(\mathbf{r}, t) = \omega_0(\mathbf{r}, t)e^{-t/\text{Re}_\lambda}$, with $\mathbf{r} = (x, y)$ the dimensionless horizontal coordinates and t a dimensionless time. Substituting these expressions in Eq. (6.14), multiplying the full equation by e^{t/Re_λ} and rescaling time to $t_* = \text{Re}_\lambda(1 - e^{-t/\text{Re}_\lambda})$ the following equation is obtained:

$$\frac{\partial \omega_0}{\partial t_*} + (\mathbf{v}_0 \cdot \nabla) \omega_0 = \frac{1}{\text{Re}_*} \nabla^2 \omega_0, \quad (6.17)$$

with a renormalized Reynolds number, $\text{Re}_* = e^{-t/\text{Re}_\lambda} \text{Re}$. Note that this renormalized equation, first proposed by Hansen et al. (1998), is similar to the traditional 2D vorticity equation for $t \lesssim \text{Re}_\lambda$ as then $t_* \approx t$. Moreover, $\lim_{\lambda \rightarrow 0} t_* = t$. With this renormalization 2D decaying flows with bottom friction behave as purely 2D decaying flows, but with a time-dependent Reynolds number, which can only evolve for a finite time (as $t_* \leq \text{Re}_\lambda$).

Clercx et al. (2003) have tested the validity of the renormalized vorticity equation for a range of Re_λ in numerical simulations, and for a range of fluid-layer depths in laboratory experiments. Numerical simulations with initial integral-scale Reynolds numbers of 1000, 2000 and 5000 with $Re_\lambda \in \{10, 20, 25, 33, 50, 100, \infty\}$ clearly show bottom-friction independent time evolution of the compensated energy $E_0(t)$ and for the compensated enstrophy $\Omega_0(t)$. For each Re the curves for different Re_λ collapse on each other, thus have the same scaling exponents independent of Re_λ . The scaling exponents of the average vortex radius, the mean vortex separation, the averaged normalized vorticity extremum, and the density of vortices, as obtained in our numerical simulations (all key quantities in the analysis by Carnevale et al. (1991), Carnevale et al. (1992)), turn out to be independent of bottom friction.

The analysis of data from laboratory experiments in shallow fluid layers (Clercx et al. 2003) reveals a more mixed picture. The experiments have been carried out in a container of horizontal dimensions of 52×52 cm, the diameter of the magnets is 25 mm and the magnets are positioned on a 10×10 chess-board-like pattern (minimum distance between the magnet centers is 50 mm). The fluid layer depth H is varied between 4 and 12 mm. The value of the Rayleigh friction λ can be estimated by the expression $\lambda = \frac{\pi^2 \nu}{4H^2}$. In these experiments, it is found that global quantities like $E_0(t)$, $\Omega_0(t)$, the average length scale l in the flow estimated by $l \approx \sqrt{E_0(t)/\Omega_0(t)}$ and the normalized vorticity extremum, $\omega_{ext}/\sqrt{E(t)}$ are virtually independent of the fluid layer depth (and in agreement with an earlier experiment by Danilov *et al.* (2002) which have been carried out with fluid layer depths of 2–6 mm). The experimental data for the average vortex density $\rho(t)$ and average vortex radius $r(t)$ are less conclusive. Power-law exponents are found for small fluid layer depths ($H \leq 8$ mm) that are in agreement with earlier reported results by Cardoso et al. (1994), but significantly larger power-law exponents are measured in the experiments with fluid layer depths between 8 and 12 mm. This would suggest that for integral quantities like the (compensated) energy and enstrophy the model of 2D turbulence with Rayleigh damping is a suitable model also implying that these integral quantities are not very sensitive to secondary 3D flow structures in shallow fluid layers. However, for the vortex statistics quantities like vortex density, vortex size and vortex separation the 2D flow model with Rayleigh damping does not provide a complete description.

6.5.3 Secondary Flows in Quasi-2D Turbulence in Thin Fluid Layers

During the last decade more attention has been paid to the influence of secondary 3D recirculations in shallow fluid layer experiments. The first detailed measurements were conducted by Akkermans et al. (2008a, b, 2010). Based on stereoscopic PIV and 3D numerical simulations, they analyzed the flow field within dipolar vortex structures in shallow fluid layers, with emphasis on the out-of-plane (vertical) velocity component. These stereoscopic PIV measurements have shown the presence of

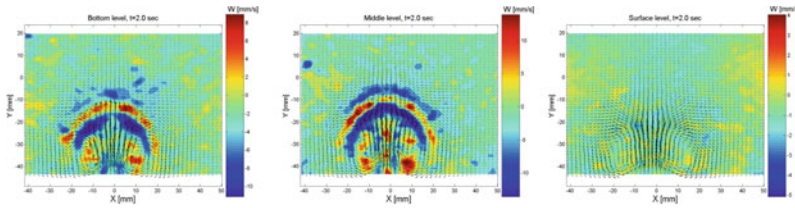


Fig. 6.8 Instantaneous velocity fields of a dipolar vortex in a horizontal plane by stereoscopic PIV measurements. The panels, from left to right, represent the flow near the bottom plate, at half height in the fluid layer and near the free surface, respectively. Vectors represent the horizontal velocity components (typically with a magnitude of a few cm/s in the vortex core) and the colors indicate the magnitude of the vertical velocity (5–10 mm/s). Courtesy Rinie Akkermans and Fluid Dynamics Laboratory, TU Eindhoven

significant, persistent (in time) and complex 3D flow structures, see the stereoscopic PIV data shown in Fig. 6.8. Full 3D numerical simulations revealed flow patterns with significant vertical motion largely consistent with the experimental data. Quite surprisingly, the flow patterns and out-of-plane motion appear independent of the applied boundary condition at the bottom, no-slip or stress-free. This might hint at the fact that bottom friction is not solely responsible for the 3D secondary flows, but it is basically vertical confinement and associated vertical gradients in the horizontal velocity field due to the boundary conditions; see Akkermans et al. (2008a) for an in-depth discussion. By measuring vertical slices of the horizontal motion in the fluid layer it became clear that a Poiseuille-like profile for the vertical variation of the horizontal velocity field is completely absent, both in experiments and in simulations. These conclusions are supported by the use of a global indicator of (lack of) two-dimensionality: the normalized horizontal divergence measured at several heights in the fluid layer,

$$\Lambda = \frac{H \int_{\mathcal{D}} |\nabla \cdot \mathbf{v}| dA}{L \int_{\mathcal{D}} |\omega_z| dA}. \tag{6.18}$$

Here, \mathbf{v} is once again the horizontal velocity field (u, v), and ∇ represent the horizontal gradient operator. This measure clearly gives significant non-zero values (while for 2D flows it should be zero). For further discussions, see Albagnac et al. (2011), Duran-Matute et al. (2010, 2011, 2012).

The question is then if the degree of two-dimensionality can be improved through the use of a two-fluid-layer configuration. The finding that the 3D secondary flows in shallow fluid layers are due to vertical confinement and associated vertical gradients in the horizontal velocity field immediately implies that application of a stratified shallow two-layer system, aimed at reducing the effect of bottom friction, will not suppress out-of-plane motions significantly. A different set of experiments and simulations by Akkermans et al. (2010) has confirmed this conjecture. Two recent studies came with further supporting evidence, see Kelley and Ouellette (2011) for two-layer stratified shallow flows, and (Tithof et al. 2018). In this latter work the authors

compared three kinds of shallow flow experiments: a single fluid layer, a miscible two-layer system, and an immiscible two-layer system. They do not have access to all three components of the velocity field but used instantaneous 2D (horizontal) flow fields and quantified the out-of-plane motion using an approach from physical oceanography. The horizontal flow field is projected onto a stream function, boundary and potential modes, see for details (Kelley and Ouellette 2011), providing an alternative global indicator for two-dimensionality. This global indicator and the one in Eq. (6.18) resulted in similar conclusions with regard to how well two-dimensionality is or is not satisfied. Their conclusion, in agreement with those by Akkermans et al. (2008a, 2010), is basically that comparable levels of out-of-plane motion are measured for the single-layer case and the immiscible two-layer case, bringing strong doubt into the standard assumption since the 1990s that stratification enhances two-dimensionality.

6.5.4 *Concluding Remarks*

From this overview, it is important to realize that imposing a parameterization of bottom friction provides good results with regard to several global quantities, like the energy and enstrophy of the flow. However, they provide only a very qualitative description of the influence of 3D secondary flows (and do not cover the sources of it). Even a global measure as the averaged horizontal divergence is of limited value and deeper insight into the flow dynamics itself is required, for example, to understand what happens for flows in thin two-layer stratified fluids. This is still a matter of research. Several critical aspects with regard to quasi-2D flows in (stratified) shallow fluid layers need to be understood better. This kind of experiments nevertheless have provided useful insights with regard to the dynamics of 2D turbulence in the last few decades and we expect they continue to do so.

6.6 Summary

This chapter started with the observation that flows in thin fluid layers, like in the atmosphere of the Earth or in the oceans or coastal seas tend to behave quasi-two-dimensional under certain conditions. Several phenomena in such systems such as the formation and evolution of large-scale coherent structures, interaction of the flow with coastal boundaries, confinement effects, etc. can, at least partly, be comprehended with basic processes relevant in 2D fluid dynamics and, more specifically, 2D turbulence. In this chapter, the basic processes relevant for 2D turbulence have been reviewed with emphasis on a phenomenological description of these processes. With the applications in mind the role of horizontal confinement on flow organization is discussed and the role of lateral walls as vorticity source is highlighted. It describes processes that finds its counterparts in the oceans and coastal seas, see

Fig. 6.1 as one typical example. Finally, the use of laboratory set-ups to study such flows has been discussed in Sects. 6.3.2 and 6.5. I believe that the huge amount of knowledge collected in the last 50 years from fundamental 2D turbulence studies in general, but also the impact of lateral and bottom boundaries on their dynamics, and the quasi-2D behavior of such systems can contribute to our understanding of large-scale geophysical flows. This is a good example how numerical simulations and laboratory experiments of model systems can contribute to our understanding of geophysical systems.

Acknowledgements HJHC gratefully acknowledge financial support for the 2D Turbulence program from the Nederlandse Organisatie voor Wetenschappelijk Onderzoek I (NWO-I), the Netherlands (formerly known as Stichting voor Fundamenteel Onderzoek der Materie, FOM). The author would like to thank Dr. Matias Duran-Matute from Eindhoven University of Technology for carefully reading the manuscript and providing many suggestions for improvement.

References

- Akkermans, R.A.D., A.R. Cieslik, L.P.J. Kamp, R.R. Trieling, H.J.H. Clercx, and G.J.F. Van Heijst. 2008. The three-dimensional structure of an electromagnetically generated dipolar vortex in a shallow fluid layer. *Physics Fluids* 20: 116601.
- Akkermans, R.A.D., L.P.J. Kamp, H.J.H. Clercx, and G.J.F. Van Heijst. 2008. Intrinsic three-dimensionality in electromagnetically driven shallow flows. *Europhysics Letters* 83: 24001.
- Akkermans, R.A.D., L.P.J. Kamp, H.J.H. Clercx, and G.J.F. Van Heijst. 2010. Three-dimensional flow in electromagnetically driven shallow two-layer fluids. *Physical Review E* 82: 026314.
- Albagnac, J., L. Lacaze, P. Brancher, and O. Eiff. 2011. On the existence and evolution of a spanwise vortex in laminar shallow water dipoles. *Physics of Fluids* 23: 086601.
- Basdevant, C., B. Legras, and R. Sadourny. 1981. A study of barotropic model flows: Intermittency, waves and predictability. *Journal of Atmospheric Sciences* 38: 2305–2326.
- Batchelor, G.K. 1969. Computation of the energy spectrum in two-dimensional turbulence. *The Physics of Fluids Supply* 12: 233–239.
- Boffetta, G. 2007. Energy and enstrophy fluxes in the double cascade of two-dimensional turbulence. *Journal of Fluid Mechanics* 589: 253–260.
- Boffetta, G., and R.E. Ecke. 2012. Two-dimensional turbulence. *Annual Review of Fluid Mechanics* 44: 427–451.
- Boubnov, B.M., S.B. Dalziel, and P.F. Linden. 1994. Source-sink turbulence in a stratified fluid. *Journal of Fluid Mechanics* 261: 273–303.
- Bracco, A., J.C. McWilliams, G. Murante, A. Provenzale, and J.B. Weiss. 2000. Revisiting freely decaying two-dimensional turbulence at millennial resolution. *Physics Fluids* 12: 2931–2941.
- Buffoni, G., P. Falco, A. Griffa, and E. Zambianchi. 1997. Dispersion processes and residence times in a semi-enclosed basin with recirculating gyres: An application to the Tyrrhenian Sea. *Journal of Geophysical Research* 102: 699–713.
- Cardoso, O., D. Marteau, and P. Tabeling. 1994. Quantitative experimental study of the free decay of quasi-two-dimensional turbulence. *Physical Review E* 49: 454–461.
- Carnevale, G.F., J.C. McWilliams, Y. Pomeau, J.B. Weiss, and W.R. Young. 1991. Evolution of vortex statistics in two-dimensional turbulence. *Physical Review Letters* 66: 2735–2737.
- Carnevale, G.F., J.C. McWilliams, Y. Pomeau, J.B. Weiss, and W.R. Young. 1992. Rates, pathways, and end states of nonlinear evolution in decaying two-dimensional turbulence: Scaling theory versus selective decay. *Physics Fluids A* 4: 1314–1316.

- Carnevale, G.F., O.U. Velasco Fuentes, and P. Orlandi. 1997. Inviscid dipole-vortex rebound from a wall or coast. *Journal of Fluid Mechanics* 351: 75–103.
- Chavanis, P.H., and J. Sommeria. 1996. Classification of self-organized structures in two-dimensional turbulence: The case of a bounded domain. *Journal of Fluid Mechanics* 314: 267–297.
- Chen, D., and G.H. Jirka. 1995. Experimental study of plane turbulent wakes in a shallow water layer. *Fluid Dynamics Research* 16: 11–41.
- Clercx, H.J.H., and G.J.F. van Heijst. 2002. Dissipation of kinetic energy in two-dimensional bounded flows. *Physical Review E* 65: 066305.
- Clercx, H.J.H., and G.J.F. van Heijst. 2009. Two-dimensional Navier-Stokes turbulence in bounded domains. *Applied Mechanics Reviews* 62: 020802.
- Clercx, H.J.H., and G.J.F. van Heijst. 2017. Dissipation of coherent structures in confined two-dimensional turbulence. *Physics of Fluids* 29: 111103.
- Clercx, H.J.H., and A.H. Nielsen. 2000. Vortex statistics for turbulence in a container with rigid boundaries. *Physical Review Letters* 85: 752–755.
- Clercx, H.J.H., S.R. Maassen, and G.J.F. van Heijst. 1998. Spontaneous spin-up during the decay of 2D turbulence in a square container with rigid boundaries. *Physical Review Letters* 80: 5129–5132.
- Clercx, H.J.H., S.R. Maassen, and G.J.F. van Heijst. 1999. Decaying two-dimensional turbulence in square containers with no-slip or stress-free boundaries. *Physics of Fluids* 11: 611–626.
- Clercx, H.J.H., A.H. Nielsen, D.J. Torres, and E.A. Coutsias. 2001. Two-dimensional turbulence in square and circular domains with no-slip walls. *European Journal of Mechanics B Fluids* 20: 557–576.
- Clercx, H.J.H., G.J.F. van Heijst, and M.L. Zoetewij. 2003. Quasi-two-dimensional turbulence in shallow fluid layers: The role of bottom friction and fluid layer depth. *Physical Review E* 67: 066303.
- Colin de Verdière, A. 1980. Quasi-geostrophic turbulence in a rotating homogeneous fluid. *Geophysical and Astrophysical Fluid Dynamics* 15: 213–251.
- Couder, Y. 1984. Two-dimensional grid turbulence in a thin liquid film. *Journal der Physique Letters* 45: L353–L360.
- Danilov, S.D., and D. Gurarie. 2000. Quasi-two-dimensional turbulence. *Physics Uspekhi* 43: 863–900.
- Danilov, S., F.V. Dolzhanskii, V.A. Dovzhenko, and V.A. Krymov. 2002. Experiments on free decay of quasi-two-dimensional turbulent flows. *Physical Review E* 65: 036316.
- Dolzhanskii, F.V., V.A. Krymov, and DYu. Manin. 1992. An advanced experimental investigation of quasi-two-dimensional shear flows. *Journal of Fluid Mechanics* 241: 705–722.
- Duran-Matute, M., J. Albagnac, L.P.J. Kamp, and G.J.F. van Heijst. 2010. Dynamics and structure of decaying shallow dipolar vortices. *Physics of Fluids* 22: 116606.
- Duran-Matute, M., R.R. Trieling, and G.J.F. van Heijst. 2011. Scaling and asymmetry in an electromagnetically forced dipolar flow structure. *Physical Review E* 83: 016306.
- Duran-Matute, M., L.P.J. Kamp, R.R. Trieling, and G.J.F. van Heijst. 2012. Regimes of two-dimensionality of decaying shallow axisymmetric swirl flows with background rotation. *Journal of Fluid Mechanics* 691: 214–244.
- Falco, P., A. Griffo, P.-M. Poulain, and E. Zambianchi. 2000. Transport properties in the Adriatic Sea as deduced from drifter data. *Journal of Physical Oceanography* 30: 2055–2071.
- Fang, L., and N.T. Ouellette. 2017. Multiple stages of decay in two-dimensional turbulence. *Physics of Fluids* 29: 111105.
- Fincham, A.M., T. Maxworthy, and G.R. Spedding. 1996. Energy dissipation and vortex structure in freely decaying, stratified grid turbulence. *Dynamics of Atmospheres and Oceans* 23: 155–169.
- Fjørtoft, R. 1953. On the changes in the spectral distribution of kinetic energy for two-dimensional non-divergent flow. *Tellus* 5: 69–74.
- Fornberg, B. 1977. Numerical study of 2-D turbulence. *Journal of Computational Physics* 25: 1–31.

- Hansen, A.E., D. Marteau, and P. Tabeling. 1998. Two-dimensional turbulence and dispersion in a freely decaying system. *Physical Review E* 58: 7261–7271.
- Hopfinger, E.J., F.K. Browand, and Y. Gagne. 1982. Turbulence and waves in a rotating tank. *Journal of Fluid Mechanics* 125: 505–534.
- Jirka, G.H. 2001. Large scale flow structures and mixing processes in shallow flows. *Journal of Hydraulic Research* 39: 567–573.
- Kato, T. 1984. Remarks on zero viscosity limit for nonstationary Navier-Stokes flows with boundary. In *Proceedings of the seminar on nonlinear partial differential equations*, pp. 85–98, MRSI, Berkely.
- Keetels, G.H., H.J.H. Clercx, and G.J.F. van Heijst. 2010. On the origin of spin-up processes in decaying two-dimensional turbulence. *European Journal of Mechanics B Fluids* 29: 1–8.
- Keetels, G.H., W. Kramer, H.J.H. Clercx, and G.J.F. van Heijst. 2011. On the Reynolds number scaling of vorticity production at no-slip walls during vortex-wall collisions. *Theoretical and Computational Fluid Dynamics* 25: 293–300.
- Kellay, H., and W.I. Goldburg. 2002. Two-dimensional turbulence: A review of some recent experiments. *Reports on Progress in Physics* 65: 845–894.
- Kellay, H., X.L. Wu, and W.I. Goldburg. 1995. Experiments with turbulent soap films. *Physical Review Letters* 74: 3975–3978.
- Kelley, D.H., and N.T. Ouellette. 2011. Onset of three-dimensionality in electromagnetic thin-layer flows. *Physics of Fluids* 23: 045103.
- Kraichnan, R.H. 1967. Inertial ranges in two-dimensional turbulence. *Physics of Fluids* 10: 1417–1423.
- Kraichnan, R.H. 1971. Inertial-range transfer in two and three-dimensional turbulence. *Journal of Fluid Mechanics* 47: 525–535.
- Kramer, W., H.J.H. Clercx, and G.J.F. van Heijst. 2007. Vorticity dynamics of a dipole colliding with a no-slip wall. *Physics of Fluids* 19: 126603.
- Legras, B., P. Santangelo, and R. Benzi. 1988. High-resolution numerical experiments for forced two-dimensional turbulence. *Europhysics Letters* 5: 37–42.
- Leith, C.E. 1968. Diffusion approximation for two-dimensional turbulence. *Physics of Fluids* 11: 671–673.
- Li, S., and D. Montgomery. 1996. Decaying two-dimensional turbulence with rigid walls. *Physics Letters A* 218: 281–291.
- Li, S., D. Montgomery, and W.B. Jones. 1997. Two-dimensional turbulence with rigid circular walls. *Theoretical and Computational Fluid Dynamics* 9: 167–181.
- Liechtenstein, L., F.S. Godeferd, and C. Cambon. 2005. Nonlinear formation of structures in rotating stratified turbulence. *Journal of Turbulence* 6: N24.
- Lilly, D.K. 1971. Numerical simulation of developing and decaying two-dimensional turbulence. *Journal of Fluid Mechanics* 45: 395–415.
- Lin, J.C., M. Ozgoren, and D. Rockwell. 2003. Space-time development of the onset of a shallow-water vortex. *Journal of Fluid Mechanics* 485: 33–66.
- Maassen, S.R., H.J.H. Clercx, and G.J.F. van Heijst. 1999. Decaying quasi-2D turbulence in a stratified fluid with circular boundaries. *Europhysics Letters* 46: 339–345.
- Maassen, S.R., H.J.H. Clercx, and G.J.F. van Heijst. 2002. Self-organization of quasi-two-dimensional turbulence in stratified fluids in square and circular containers. *Physics of Fluids* 14: 2150–2169.
- Maassen, S.R., H.J.H. Clercx, and G.J.F. van Heijst. 2003. Self-organization of decaying quasi-2D turbulence in stratified fluids in rectangular containers. *Journal of Fluid Mechanics* 495: 19–33.
- Marteau, D., O. Cardoso, and P. Tabeling. 1995. Equilibrium states of two-dimensional turbulence: An experimental study. *Physical Review E* 51: 5124–5127.
- Matthaeus, W.H., and D. Montgomery. 1980. Selective decay hypothesis at high mechanical and magnetic Reynolds numbers. *Annals of the New York Academy of Sciences* 357: 203–222.
- Matthaeus, W.H., W.T. Stribling, D. Martinez, S. Oughton, and D. Montgomery. 1991. Decaying, two-dimensional, Navier-Stokes turbulence at very long times. *Physics D* 51: 531–538.

- McWilliams, J.C. 1984. The emergence of isolated coherent vortices in turbulent flow. *Journal of Fluid Mechanics* 146: 21–43.
- Molenaar, D., H.J.H. Clercx, and G.J.F. van Heijst. 2004. Angular momentum of forced two-dimensional turbulence on a square no-slip domain. *Physics D* 196: 329–340.
- Montgomery, D., and G.R. Joyce. 1974. Statistical mechanics of negative temperature states. *Physics of Fluids* 17: 1139–1145.
- Nguyen van yen, R., M. Farge, and K. Schneider. 2011. Energy dissipating structures produced by walls in two-dimensional flows at vanishing viscosity. *Physical Review Letters* 106: 184502.
- Nguyen van yen, N., M. Waidmann, R. Klein, M. Farge, and K. Schneider. 2018. Energy dissipation caused by boundary layer instability at vanishing viscosity. *Journal of Fluid Mechanics* 849: 676–717.
- Onsager, L. 1949. Statistical hydrodynamics. *Nuovo Cimento* 6: 279–287.
- Orlandi, P. 1990. Vortex dipole rebound from a wall. *Physics of Fluids A* 2: 1429–1436.
- Paret, J., and P. Tabeling. 1998. Intermittency in the two-dimensional inverse cascade of energy: Experimental observations. *Physics of Fluids* 10: 3126–3136.
- Pointin, Y.B., and T.S. Lundgren. 1976. Statistical mechanics of two-dimensional vortices in a bounded domain. *Physics of Fluids* 19: 1459–1470.
- Proudman, J. 1916. On the motion of solids in a liquid possessing vorticity. *Proceedings of the Royal Society A* 92: 408–424.
- Rivera, M.K., and R.E. Ecke. 2005. Pair dispersion and doubling time statistics in two-dimensional turbulence. *Physical Review Letters* 95: 194503.
- Rivera, M.K., and R.E. Ecke. 2016. Lagrangian statistics in weakly forced two-dimensional turbulence. *Chaos* 26: 013103.
- Rutgers, M.A. 1998. Forced 2D turbulence: Experimental evidence of simultaneous inverse energy and forward enstrophy cascades. *Physical Review Letters* 81: 2244–2247.
- Santangelo, P., R. Benzi, and B. Legras. 1989. The generation of vortices in high-resolution, two-dimensional decaying turbulence and the influence of initial conditions on the breaking of self-similarity. *Physics of Fluids A* 1: 1027–1034.
- Schneider, K., and M. Farge. 2005. Decaying two-dimensional turbulence in a circular container. *Physical Review Letters* 95: 244502.
- Schneider, K., and M. Farge. 2008. Final states of decaying 2D turbulence in bounded domains: Influence of the geometry. *Physics D* 237: 2228–2233.
- Smith, L.M., and V. Yakhot. 1993. Bose condensation and small-scale structure generation in a random force driven 2D turbulence. *Physical Review Letters* 71: 352–355.
- Sommeria, J. 1986. Experimental study of the two-dimensional inverse energy cascade in a square box. *Journal of Fluid Mechanics* 170: 139–168.
- Sous, D., N. Bonneton, and J. Sommeria. 2004. Turbulent vortex dipoles in a shallow water layer. *Physics of Fluids* 16: 2886–2898.
- Sous, D., N. Bonneton, and J. Sommeria. 2005. Transition from deep to shallow water layer: formation of vortex dipoles. *European Journal of Mechanics-B/Fluids* 24: 19–32.
- Sutherland, D., C. Macaskill, and D.G. Dritschel. 2013. The effect of slip length on vortex rebound from a rigid boundary. *Physics of Fluids* 25: 093104.
- Tabeling, P. 2002. Two-dimensional turbulence: A physicist approach. *Physics Reports* 362: 1–62.
- Tabeling, P., S. Burkhart, O. Cardoso, and H. Willaime. 1991. Experimental study of freely decaying two-dimensional turbulence. *Physical Review Letters* 67: 3772–3775.
- Taylor, G.I. 1917. Motions of solids in fluids when the flow is not irrotational. *Proceedings of the Royal Society* 93: 99–113.
- Tithof, J., B.C. Martell, and D.H. Kelley. 2018. Three-dimensionality of one- and two-layer electromagnetically driven thin-layer flows. *Physical Review Fluids* 3: 064602.
- Uijttewaal, W.S.J. 2014. Hydrodynamics of shallow flows: Application to rivers. *Journal of Hydraulic Research* 52: 157–172.
- Uijttewaal, W.S.J., and R. Booij. 2000. Effects of shallowness on the development of free-surface mixing layers. *Physics of Fluids* 12: 392–402.

- Uijttewaal, W.S.J., and G.H. Jirka. 2003. Grid turbulence in shallow flows. *Journal of Fluid Mechanics* 489: 325–344.
- Van Heijst, G.J.F., and H.J.H. Clercx. 2009. Laboratory modeling of geophysical vortices. *Annual Review of Fluid Mechanics* 41: 143–164.
- Van Heijst, G.J.F., H.J.H. Clercx, and D. Molenaar. 2006. The effects of solid boundaries on confined two-dimensional turbulence. *Journal of Fluid Mechanics* 554: 411–431.
- Weiss, J.B., and J.C. McWilliams. 1993. Temporal scaling behavior of decaying two-dimensional turbulence. *Physics of Fluids A* 5: 608–621.
- Wells, J., and Ya..D.. Afanasyev. 2004. Decaying quasi-two-dimensional turbulence in a rectangular container: Laboratory experiments. *Geophysical and Astrophysical Fluid Dynamics* 98: 1–20.
- Yap, C.T., and C.W. van Atta. 1993. Experimental studies of the development of quasi-two-dimensional turbulence in stably stratified fluid. *Dynamics of Atmospheres and Oceans* 19: 289–323.